

# Permeability enhancement performance and its control factors by auger mining of extremely thin coal seams

Yong Yuan<sup>1,2</sup>, Zhongshun Chen<sup>1,2,3,4</sup>, Chaoshui Xu<sup>3</sup>, Xinwang Zhang<sup>1,2</sup> and Hongmin Wei<sup>1,2</sup>

<sup>1</sup>School of Mines, Key Laboratory of Deep Coal Resource, Ministry of Education of China, China University of Mining & Technology, Xuzhou, Jiangsu 221116, People's Republic of China

<sup>2</sup>The State Key Laboratory of Coal Resources and Safe Mining, China University of Mining & Technology, Xuzhou, Jiangsu 221116, People's Republic of China

<sup>3</sup>School of Civil, Environmental and Mining Engineering, The University of Adelaide, South Australia, 5005, Australia

E-mail: [chenzhongshun2016@163.com](mailto:chenzhongshun2016@163.com)

Received 16 April 2018, revised 24 August 2018

Accepted for publication 11 September 2018

Published 16 October 2018



CrossMark

## Abstract

In order to improve both the pressure relief in deep coal mining and the permeability of coal seams for gas drainage, the auger mining (AM) method was proposed for mining extremely thin coal seams underneath a major coal seam to enhance its permeability and improve its pressure relief for subsequent major mining. The method was applied to Chiyu Coal Mine in China as a case study. Based on the geological conditions of the mine, the influences of AM parameters such as AM width, intermediate coal pillar width and distance between adjacent temporary wide pillars on the pressure distributions and permeability enhancement were studied in detail and the optimal set of parameters for the mining operation were obtained. Based on our simulations, it was found that using the proposed method with the optimal parameters derived, the permeability of the upper protected coal layer will increase by more than 671 times the initial permeability. This demonstrated that the proposed new AM method is effective for the purposes of pressure relief and permeability enhancement in the protected major coal layer.

Keywords: extremely thin coal seams, permeability enhancement, auger mining, temporary wide pillars, intermediate coal pillar

(Some figures may appear in colour only in the online journal)

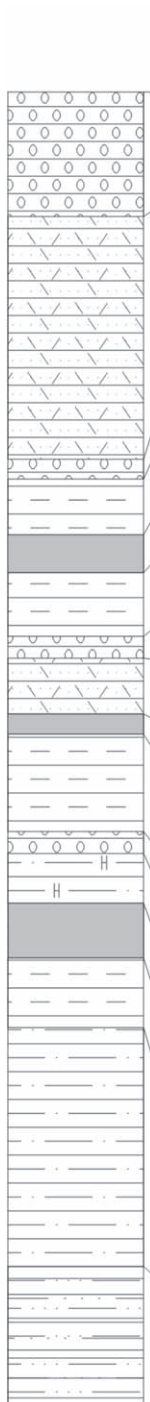
## 1. Introduction

The proven coal resource buried at the depth of more than 1000 m accounts for about 53% of the total coal resource in China (Peng 2008). The mining at such significant depth is often associated with complex and harsh conditions such as high stress, high ground temperature, high karst water pressure and severe mining disturbance, resulting in high potential of coal and gas outburst, rock burst and other related disasters (Ranjith *et al* 2017, Zhou *et al* 2017). In these cases, mining lower protective layers to relieve the high pressure and enhance the

permeability of the upper protected major coal layers to be mined later has proved to be an effective way for safe and efficient mining of these deep coal resources (Aguado and Nicieza 2007, Jin *et al* 2016). In addition, based on Chinese Coal Mine Safety Regulations, the mining techniques using protective layers must be implemented for regional pressure relief when mining outburst-prone coal seams. Therefore, it is important to understand the mechanism of pressure relief and permeability enhancement of the protected layers in deep mining, so that operations can be designed and managed properly when practically implemented.

There are numerous published research on protective layer mining mechanism within the context of fully mechanized longwall mining (FMLM) (Fang *et al* 2009, Liu *et al* 2011,

<sup>4</sup> Author to whom any correspondence should be addressed.



Thickness	Lithology	Characterization
6.25	Medium fine sandstone	Gray-green, medium-thick layered, quartz-based, lithic debris followed by poor sorting, complex filling, uniform bedding, large-scale cross-bedding.
12.2	Siltstone	Grayish green siltstone, horizontal texture development.
1.0	Medium fine sandstone	Thin bedding, interbedded with mudstone strips, a large number of plant fossil fragments, large-scale cross-bedding, vein-like, wavy bedding
2.8	Mudstone	Dark gray, black, gray, medium thick layered, rich in plant fossils, locally containing a small amount of siderite nodules.
1.9	2# coal	Black, weak glass lustre, banded structure, bright coal.
3.2	Mudstone	Thin layer, horizontal texture, rich plant fossils, lower often contain iron ore nodules.
1.1	Medium fine sandstone	Thin layer, wavy, veined bedding.
2.8	Siltstone	A layer of unstable middle fine grained sandstone is mainly sandwiched in the middle layer.
1.0	3# coal	Black, weak glass lustre, banded structure, bright coal.
4.89	Mudstone	Grayish black, dark gray, with horizontal texture and wavy, lobed bedding.
1.1	Medium fine sandstone	Thin bedding, interbedded with mudstone strips, a large number of plant fossil fragments, large-scale cross-bedding, vein-like, wavy bedding.
2.5	Carbonaceous mudstone	Grayish black, dark gray. It consists of 0-2 layers of light gray thin thin middle fine sandstone, with horizontal texture and wavy, lobed bedding.
2.76	4# coal	Black, luster is dark. The main ingredient is bright coal.
3.5	Mudstone	Medium - thin layer, containing plant fossils, partly containing siderite nodules.
12.0	Sandy mudstone	Lamellar, wavy, veined bedding.
7.0	Siltstone	Thin middle thick layered, locally pyrite bearing brachiopod fossils.

Figure 1. Drill hole columnar section.

Yang et al 2011, Chen et al 2013, Wang et al 2013a, Zhang et al 2015), but very little work has been done in the area of auger mining (AM). The thickness of the coal seam in the FMLM face must normally be more than 1.2 meters so as to avoid excessive waste rock production (Song and Yun 2013). In other words, the FMLM method is not suitable if the thickness of the coal seam to be mined is less than 1.0 meter (Yan and Miao 2009). If the FMLM method was used in this case, in addition to excessive waste, the mining may also cause excessive

damage to the roof or floor layers, which will result in large strata movement and increase the risk of rock outburst or water inrush (Tang 2015, Xiong et al 2015). AM is suitable for a coal seam where the surrounding rock is stable and the inclination of the coal seam varies little. A drawback is that coal production is small due to the thin coal seam and it takes a long time for handling the drill pipe. However, in the situation of mining extremely thin coal seams, it will be advantageous to use the AM method as the benefits include a simple mining layout, less

equipment required and easier automation. At present, the application of the AM method for permeability enhancement and pressure relief in the protected layer still remains challenging and the mechanism is far from fully understood.

In this paper, a method is proposed for the analysis of pressure relief and permeability enhancement in the protected layers when AM is used to mine the protective layer underneath. The effects of pressure relief and permeability enhancement at different AM parameters are discussed in detail, which provides useful references and examples for the implementation of the AM method in practice.

## 2. AM method for mining extremely thin protective coal seams

### 2.1. Geological conditions

Chiyu Coal Mine is a high gassy mine with the design production capacity of 3.0 Mt/a. The main mineable coal seams of North No. 3 panel are the 2# and 3# of the Shanxi Formation. The average thickness of the 2# and 3# coal seam is 1.9 and 1.0 m with the interlayer spacing of 7.1 m. The drill hole columnar section is shown in figure 1.

Due to small interlayer spacing, high gas pressure and low permeability, the drainage of gas was carried out beforehand at the coal mine by driving a rock roadway in the floor of 3# coal seam, which led to a great number of drill holes but a poor effect. Therefore, the protective mining method was proposed, and 3# coal seam was selected as the protective layer because of its low gas pressure, small thickness, small absolute gas content and low probability of gas accident. However, if we had set a longwall mining face in 3# coal seam, the 2# coal seam would collapse to the goaf of 3# coal seam. Therefore, we proposed to excavate the 3# coal seam with the AM method, which required the understanding of the permeability evolution law with AM in an extremely thin protective layer to guide the gas drainage in practice.

### 2.2. Conventional AM face

In an AM face, the cutting heads are arranged in the roadway where the workers operate the machine to mine the coal seam. Drill bits are pushed in a longitudinal direction to mine the coal, which is then conveyed along the drill pipes to the scraper conveyor. Intermediate coal pillars (ICPs) are left between the AM rooms. The layout of a typical AM face and its mining process are shown in figure 2.

Excavations inevitably will cause pressure redistribution in the surrounding rocks and permeability enhancement due to strata movement, formation of rock fractures and rock breakage (Wang *et al* 2013b, Liu and Cheng 2015, Yao *et al* 2016). This can benefit the gas drainage in the surrounding rocks. The size of the excavation determines the range of rock failure and the magnitude of strata movement, stress and permeability changes (Zhang *et al* 2016a). For conventional AM, significant pressure relief and permeability

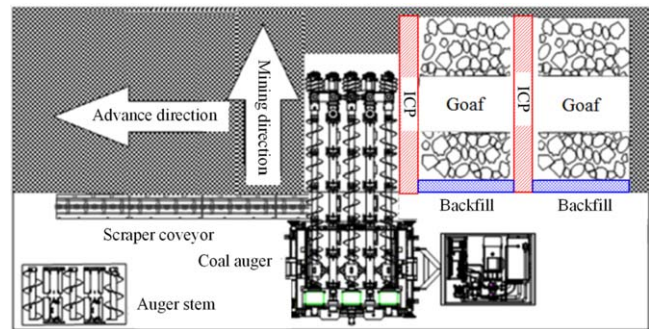


Figure 2. Layout of a conventional AM face.

enhancement are hard to achieve due to the small mining rooms and the arrangement of the ICPs.

### 2.3. Proposed AM method for effective pressure relief and permeability enhancement

In order to improve the effects of pressure relief and permeability enhancement within rocks above the AM excavations, a novel method of AM of extremely thin coal seams is proposed. The flowchart shown in figure 3 gives detailed steps to follow for the optimization of the operational parameters for this mining method.

Compared with the conventional AM method, the key to the proposed method is to increase the AM room width and reduce the ICP width so that effective strata movement can be achieved, while ensuring safe mining operations. The ICPs in this case are designed to provide only short-term temporary support of the AM rooms and they are designed to collapse under the strata pressure after the coal auger moves to the next AM room. This increased roof failure will accelerate the effects of pressure relief and permeability enhancement for the coal seams above. To ensure a safe working environment, temporary wide pillars (TWP) are set at a certain interval to provide longer-term roof support so as to protect the coal auger from being trapped after the failures of the ICPs. The TWP can be recovered later when their protection is no longer needed. The proposed AM process is illustrated in figure 4. In this method, the degree of roof movement is the major indicator for determining whether the ICP and TWP arrangements are appropriate, which is the key to the design of a successful AM operation. The analysis of roof movement in AM and the optimization of AM operational parameters are the focus of this paper.

## 3. Design of AM parameters

The key to this proposed AM method is to control the state of the ICPs. They can provide temporary support and will collapse under the strata pressure after the AM advancing distance reaches a threshold distance. The AM width and ICP width determine the magnitude and strength of the load-bearing capacity of the coal pillar after AM, which decides the state of the ICPs and provides temporary support. With the

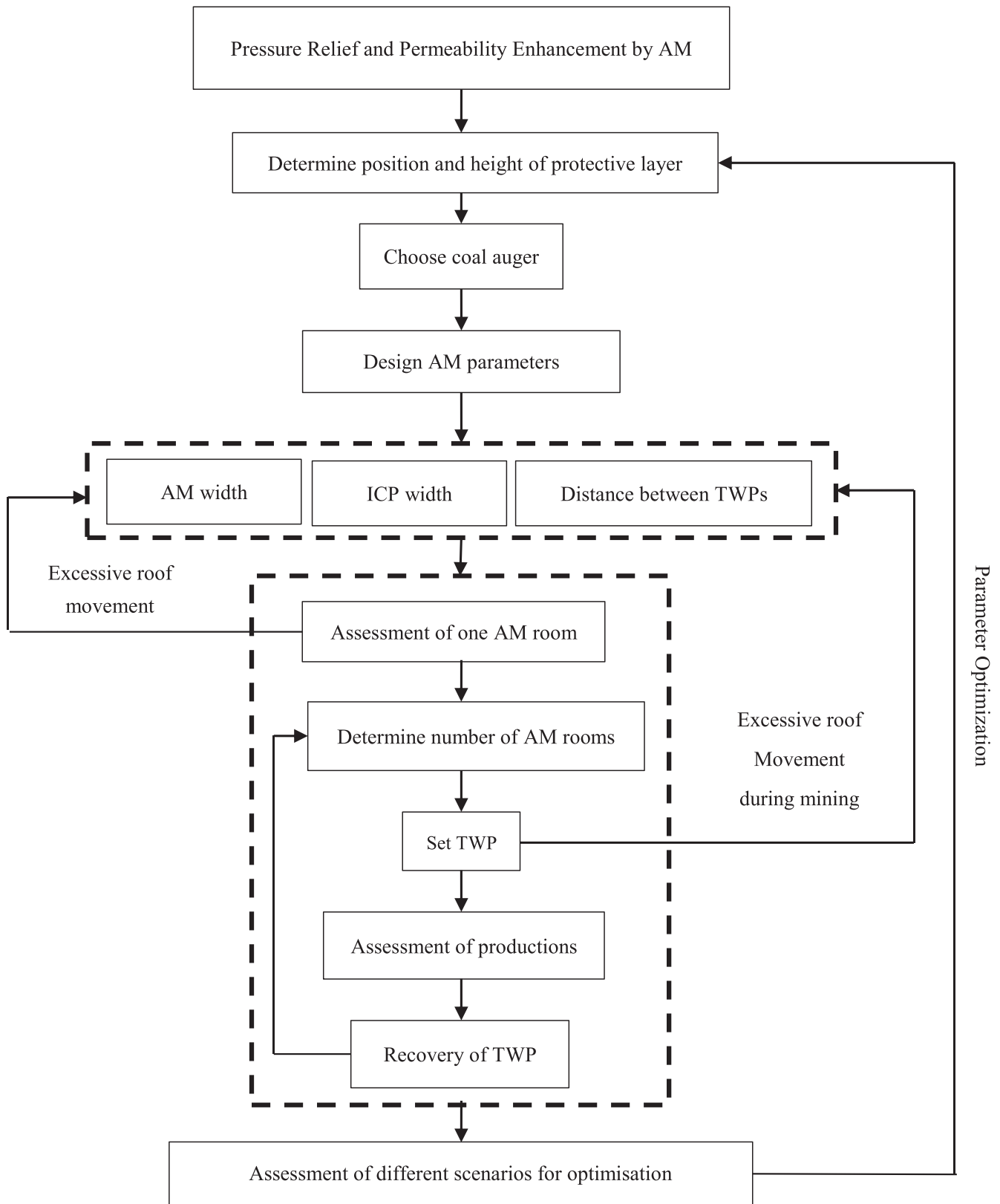


Figure 3. Flowchart for the optimization of operational parameters for the proposed AM method.

increase of mining distance, the mining area is gradually enlarged, and the ICPs behind the goaf do not need to provide support. They collapse under the strata pressure, which increases the effect of pressure relief and permeability

enhancement. Therefore, these three parameters (AM width, ICP width and the distance) are tested.

The AM model is shown in figure 5 and a simplified beam model to represent the strata of an AM room is shown

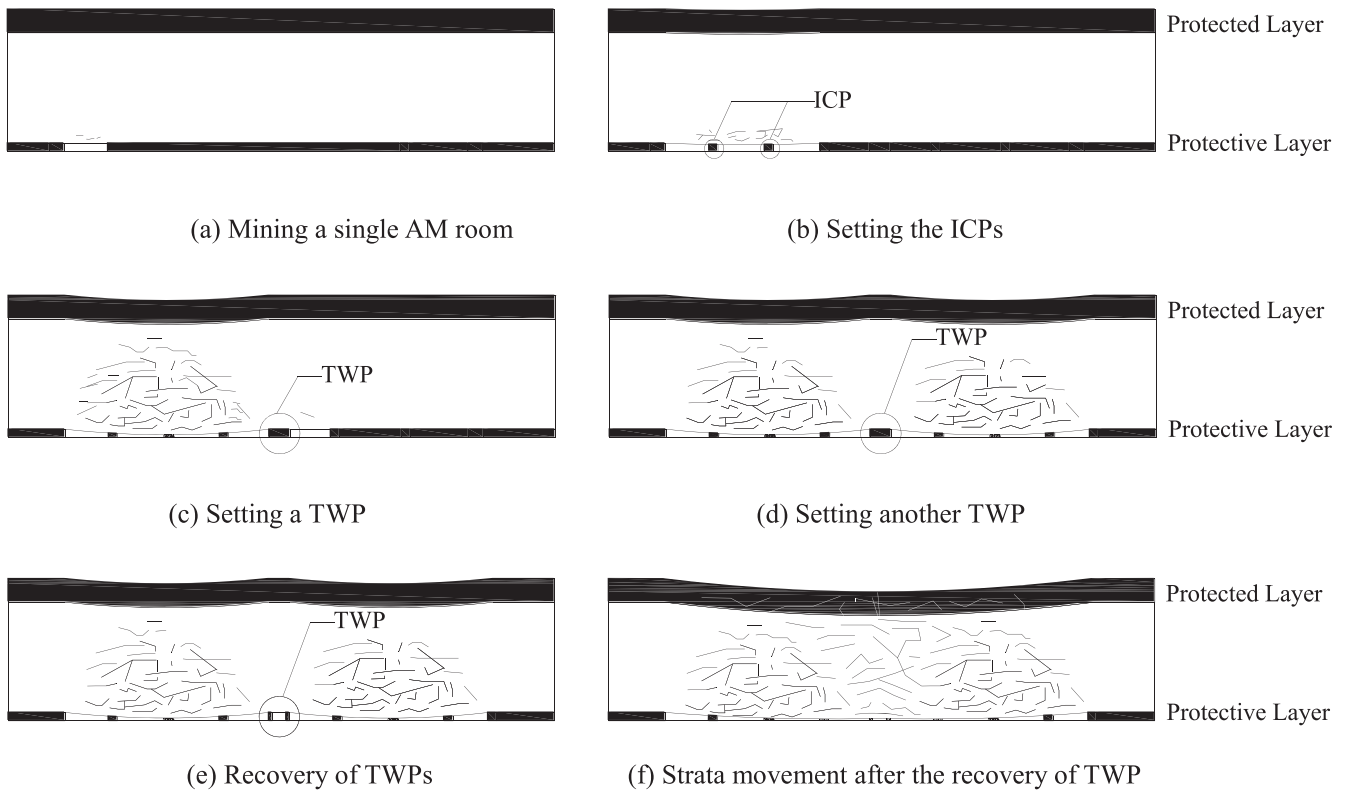


Figure 4. Schematic diagram of the proposed AM operations.

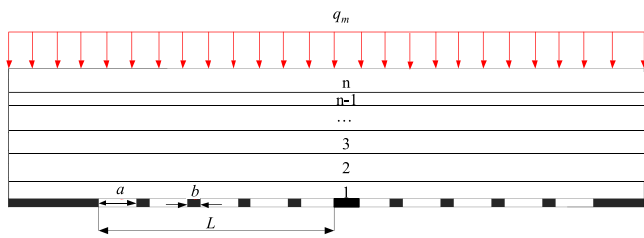


Figure 5. Representation of AM model.

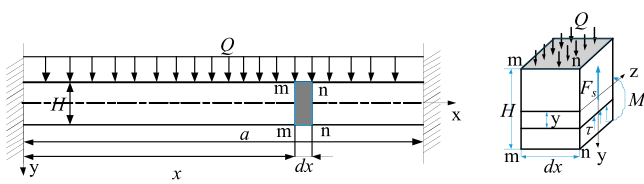
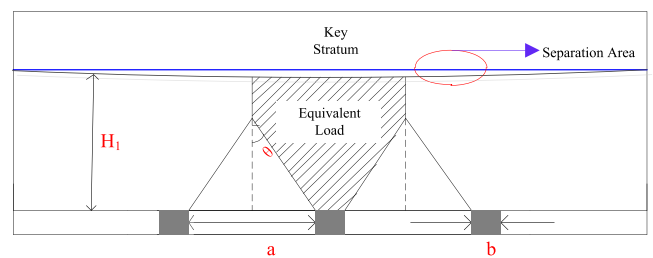


Figure 6. Model of a beam with two fixed supports.

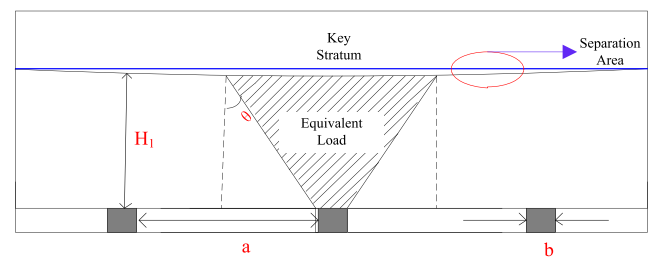
in figure 6. The parameters need to be determined include the AM width ( $a$ ), ICP width ( $b$ ) and the distance between adjacent TWPs ( $L$ ).

### 3.1. The AM width

The structure formed by AM is simplified as a beam with two fixed supports (Swift and Reddish 2002), as shown in figure 6. According to the beam theory (Chen et al 2009), the



(a)  $a \leq 2H_1 \tan \theta$



(b)  $a > 2H_1 \tan \theta$

Figure 7. Calculation of load on the ICP.

deflection in this case can be expressed as:

$$\omega = \frac{Qa^2x^2}{2EH^3} \left(1 - \frac{x}{a}\right)^2, \quad (1)$$

where  $Q$  is the vertical load above the roof strata,  $E$  is the elastic modulus of the roof,  $H$  is the thickness of the roof

strata considered and  $x$  is the distance from the left end of the beam.

During the mining of an AM room, the roof must not collapse and the roof deformation should not cause any problem for the movement of auger drills. The worst-case scenario that needs to be considered for roof movement is when the auger is mining the last section (section width =  $w$ ) of a room. In this scenario, the roof vertical displacement  $\Delta h$  at  $x = a - w$  is:

$$\Delta h = \frac{Qa^2(a-w)^2}{2EH^3} \left(1 - \frac{a-w}{a}\right)^2 = \frac{Qw^2(a-w)^2}{2EH^3}. \quad (2)$$

The AM room width can then be determined by the following formula:

$$a = w + \sqrt{\frac{2\Delta hEH^3}{Qw^2}}, \quad (3)$$

if the maximum allowable roof displacement  $\Delta h$  to ensure the safe operation of the auger drills is given.

### 3.2. The ICP width

The roof is supposed to remain stable only during the mining of the AM room. The calculation of the required ICP width is based on this requirement. It is assumed that the ICP should bear the weight of the rock below the key stratum, which is assumed to stay intact, while the rock stratum below it will separate due to ground deformation after mining, as shown in figure 7.

If  $a$  is less than  $2H_1 \tan \theta$  (in figure 7(a)), the actual load on the ICP can be calculated by the following formula:

$$\sigma_z = \sigma_{z0} \times \left(1 + \frac{a}{b}\right) - \frac{\gamma a^2}{4b} \cot \theta. \quad (4)$$

$$b = \frac{(s\sigma_{z0} - 0.64\sigma_m)h + \sqrt{(0.64h\sigma_m - s\sigma_{z0}h)^2 - s\sigma_m(0.36\gamma a^2 \cot \theta - 1.44a\sigma_{z0})h}}{0.72\sigma_m}. \quad (7)$$

Otherwise, when  $a$  is greater than  $2H_1 \tan \theta$ ,

$$b = \frac{(s\sigma_{z0} - 0.64\sigma_m)h + \sqrt{(0.64h\sigma_m - s\sigma_{z0}h)^2 + 1.44s\sigma_{z0}H_1h\sigma_m \tan \theta}}{0.72\sigma_m}. \quad (8)$$

Otherwise, if  $a$  is greater than  $2H_1 \tan \theta$  (in figure 7(b)), the load on the ICP can be calculated by the following formula:

$$\sigma_z = \sigma_{z0} \times \left(1 + \frac{H_1}{b} \tan \theta\right), \quad (5)$$

where  $\sigma_z$  is the actual load on the ICP,  $H_1$  is the thickness of the rock below the key stratum,  $\theta$  is a shear angle of rock or coal defined as  $\theta = 90^\circ - \beta$ , and  $\beta$  is the caving angle of rock or coal,  $\sigma_{z0}$  is the load below the key stratum and it is calculated as:  $\sigma_{z0} = \gamma H_1$  and  $\gamma$  is the rock bulk density.

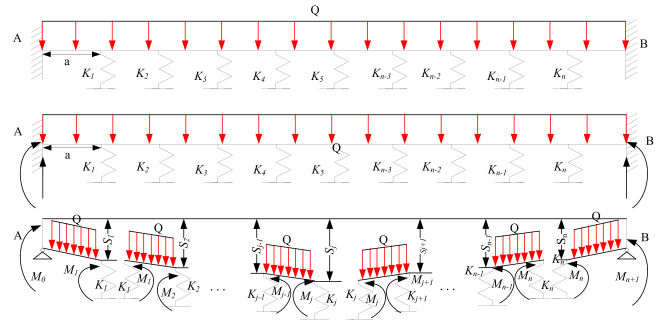


Figure 8. Model of when the ICPs are intact.

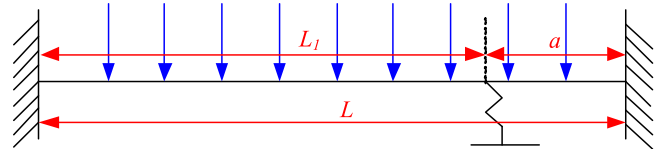


Figure 9. Model of the worst-case scenario when only one ICP support is active.

The strength of the ICP can be calculated using the following formula proposed by Bieniawski (1968):

$$\sigma_p = \sigma_m \times \left(0.64 + 0.36 \frac{b}{h}\right)^n, \quad (6)$$

where  $\sigma_p$  is the actual strength of the ICP,  $\sigma_m$  is the *in situ* coal mass strength,  $h$  is the height of the AM room and  $n = 1$  when  $b/h < 5$ . Considering a safety factor  $s$ ,  $b$  is given by the critical state when the load is equal to the strength of the ICP, i.e.  $s\sigma_z = \sigma_p$ . Therefore, if  $a$  is less than  $2H_1 \tan \theta$ ,

### 3.3. The distance between adjacent TWP

As the mining face advances, there will be additional increments for both the overburden deformation and the roof movement due to the additional stratum load created near the work face, which will increase the risk of the auger drills being trapped. TWPs are used to solve this problem and they should be placed at a certain distance apart from each other ( $L$  in figure 6) to ensure the smooth progress of the AM. To calculate an appropriate value for  $L$ , two different extreme scenarios are considered with regard to the condition of the



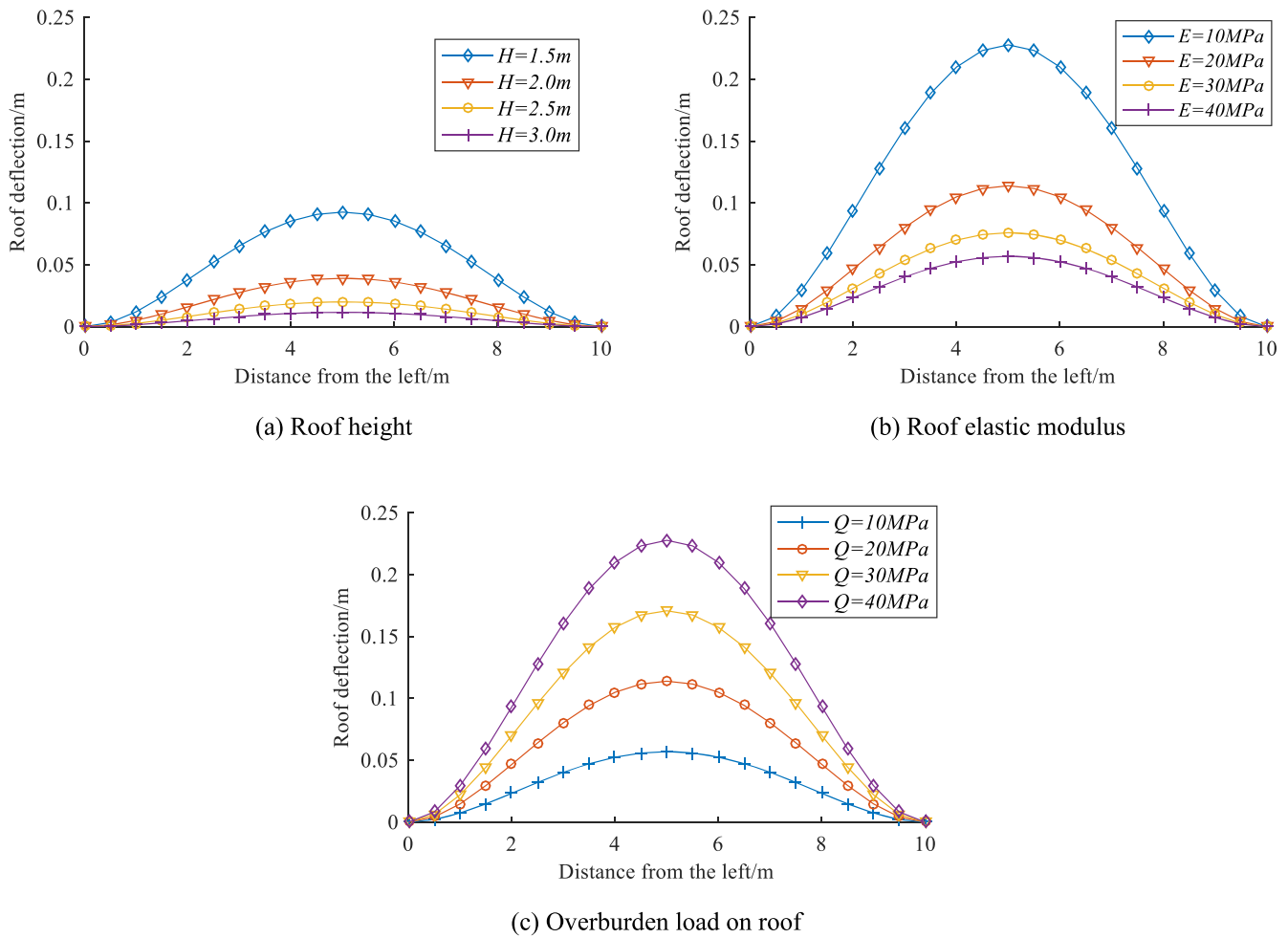


Figure 10. Influencing factors on roof deformations.

where  $\Delta h_2$  is the deformation and  $F_2$  is the force acting on the ICP caused by the part being mined.

The total deformation of the ICP  $\Delta h_3$  is the sum of  $\Delta h_1$  and  $\Delta h_2$ , i.e.

$$\Delta h_3 = \Delta h_1 + \Delta h_2 = \frac{3a^4hq}{8(a^3bk_s + 3hEI)} + \frac{3h(L - a)^4q}{8(-a^3bk_s + 3a^2bk_sL - 3abk_sL^2 + bk_sL^3 + 3hEI)}. \tag{16}$$

It is assumed that the deformation is linear in the part being mined. The width of the mining auger is  $w$  and  $\Delta h_3$  is the maximum roof deformation at distance  $a$  from the unmined coal wall (ICP in this case). Then the maximum displacement  $\Delta h$  for the worst-case scenario at the mining auger location is:

$$\Delta h = \frac{w}{a} \Delta h_3 = \frac{3a^3hqw}{8(a^3bk_s + 3hEI)} + \frac{3h(L - a)^4qw}{8(-a^3bk_s + 3a^2bk_sL - 3abk_sL^2 + bk_sL^3 + 3hEI)}. \tag{17}$$

Based on these equations, once the maximum allowable roof displacement ( $\Delta h$ ) is given, the distance  $L$  between TWPs can then be determined.

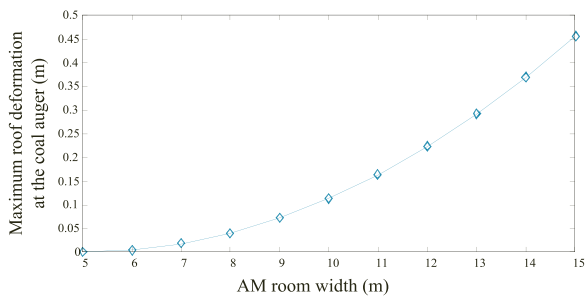
There are assumptions involved in the analytical evaluations discussed previously. Although these assumptions such as linear elastic behavior of the roof before failure and uniform roof stress may not exactly match practical conditions in some cases such as very soft roof conditions, the results do match the numerical evaluation reasonably well and a parametric study will provide some useful guidance to the optimization of AM operational parameters (see the following).

### 3.4. Parametric studies of AM variables

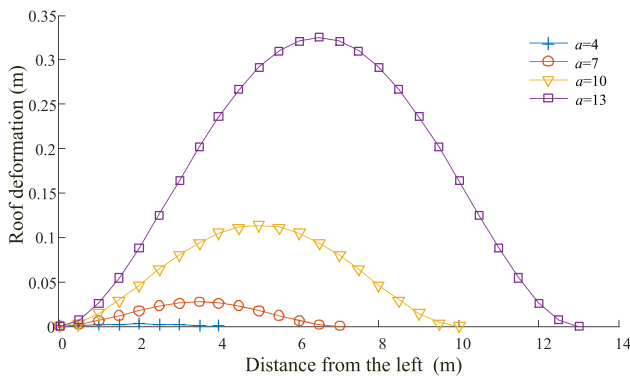
The relationships discussed above suggest that many variables will affect the roof displacement in AM. The influences of some of the key variables (height of the roof, elastic modulus and overburden load) on the roof deformation within an AM room are summarized in figure 10 when the width of AM room  $a = 10$  m, which demonstrate that:

- (1) The overall trend of variations of the roof deformation are similar, and the differences between different cases are only in their magnitude.





(a) Maximum roof deformation above the coal auger drill



(b) Roof deformation with different AM width

**Figure 11.** Relationship between AM width and roof deformation.

- (2) The greater the thickness and strength of the roof (rock beam above the mined-out area) are, the smaller the roof deflection becomes, as expected. The roof deformation increases as the overburden load increases.

Using the geological conditions of Chiyu Coal Mine and its corresponding mechanical and geometrical parameters of  $E = 20$  GPa,  $Q = 20$  MPa,  $H = 1.4$  m,  $H_1 = 80$  m and  $w = 5$  m, the relationship between the maximum roof movement at the auger location for the worst-case scenario and AM width is plotted in figure 11(a) based on equation (2), which shows a non-linear relationship. In general, for practical mining operations, a maximum roof deformation of 0.15 m near the operating rig is allowed. Based on this requirement, the AM width for the mine is determined to be less than 10 m for the case of Chiyu Coal Mine.

The overburden load is borne by the ICPs during AM operations. An ICP will fail when its strength is smaller than the load imposed by the overburden. The bearing capacity of ICPs are related to their size and strength.

Figure 12 shows the relationships between the required ICP width and AM width with different AM height and ICP strength. As expected, (1) the required ICP width increases as the AM width increases. After  $a = 2H_1 \tan \theta$ , the required ICP no longer changes; (2) the required ICP width also increases as the AM height increases; and (3) the higher the ICP strength, the smaller the required ICP width.

For the case of Chiyu Coal Mine, where  $h = 1$  m and  $\sigma_m = 20$  MPa, the required ICP width is calculated to be 2 m. If none of the ICPs fails and they are all assumed to be in the

elastic state, the roof deformation profile is shown in figure 13, where four AM rooms between a pair of TWPs are assumed. The following observations can be made:

- (1) The maximum roof deformation increases as the AM width increases.
- (2) The roof deflection is also influenced by the flexibility coefficient ( $K$ ) of ICPs. The ICPs are considered to be in a rigid state if  $K$  is 0. As expected, the greater the compliance coefficient, the greater the roof deformation under the elastic-state assumption.
- (3) The maximum roof deformation does not change as the AM work face advances, which suggests that TWPs will not make any contribution to the roof movement in the AM rooms when the ICPs are intact.

However, it is unrealistic to assume that ICPs never fail and are always in the elastic state. In fact, in the proposed AM method, all the ICPs are designed to fail under the load so as to meet the need of pressure relief and permeability enhancement. In this circumstance, according to equation (16), the relationship between the maximum roof deformation and the total AM distance between TWPs is shown in figure 14 for the case study, where the parameters used are:  $h = 1$  m,  $H_1 = 80$  m,  $\gamma = 2500$  N m<sup>-3</sup>,  $a = 10$  m and  $b = 2$  m. With the advance of the work face the maximum roof deformation reaches 0.15 m when the total AM distance reaches 40 m. Therefore, the distance between adjacent TWPs should be less than 40 m for Chiyu Coal Mine to ensure the safe operation of the auger drills.

#### 4. Numerical simulations of permeability evolution of Chiyu Coal Mine

Fast Lagrangian analysis of continua (FLAC) is used to analyze the stability of the ICP and permeability evolution of the protected layer in 3D for the Chiyu Coal Mine case study. The size of the numerical model is 140 m long, 140 m wide and 60 m high, as shown in figure 15.

The strain-softening model is applied to the protected layer and its surrounding rock and the other parts are assumed to follow the Mohr–Coulomb model. The parameters used in the simulation are shown in table 1. A vertical stress of 15 MPa is assumed at the top face of the model, while the bottom face of the model is fixed. A seepage model about stress, fracture and seepage is incorporated in the analysis. Mechanical calculation and seepage calculation are carried out separately (Zhang *et al* 2016b). The original permeability of 2# coal seam is 0.134 md.

The fracture is of importance in the evolution of permeability (Wang *et al* 2011). In the model, the permeability at different states of rock is discussed separately. The permeability within a rock mass is only related to the stress in the horizontal direction (Ren and Edwards 2002). And permeability of fractured rock is related to maximum and minimum principal stress (Durucan 1981, Zhou *et al* 2017). The fish is used in simulation to judge the state of the rock and then the

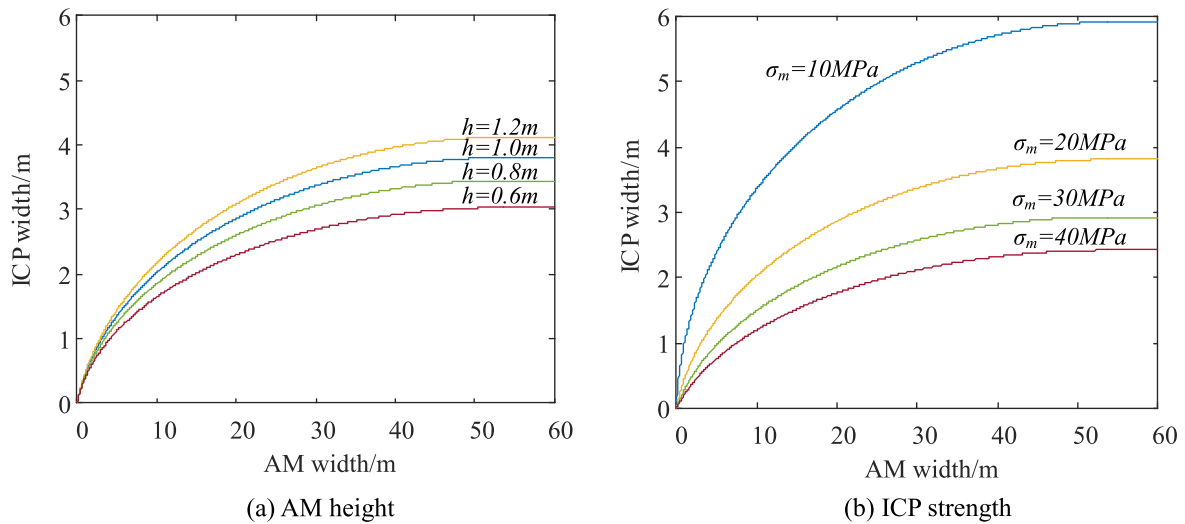
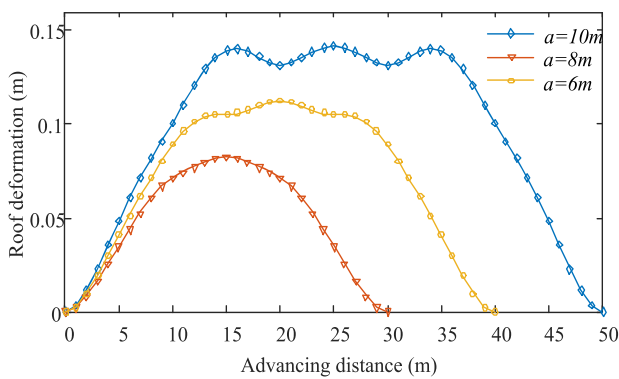
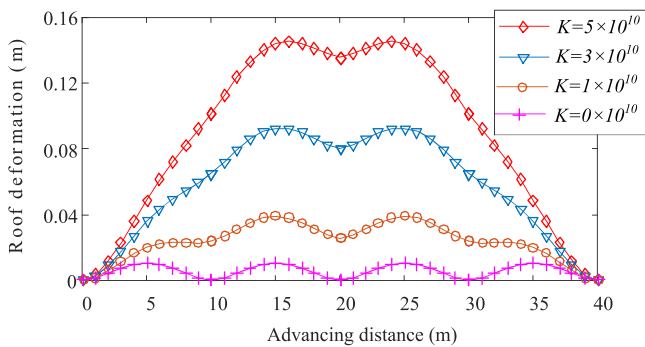


Figure 12. Relationships between the required ICP width and AM width at different conditions.



(a) At different AM width



(b) At different flexibility coefficient

Figure 13. Roof deflection profiles when the ICPs are intact.

permeability is determined by the following formula:

$$k = \begin{cases} k_0 \times e^{-0.25(\sigma_{xx} - \sigma_{xx0})}, & \text{The rock is intact.} \\ k_{f0} \times \left(\frac{\sigma_1 + \sigma_3}{2}\right)^{0.816}, & \text{The rock is fractured.} \end{cases} \quad (18)$$

where,  $k_0$  is the original permeability of rock mass,  $\sigma_{xx0}$  is the original *in situ* horizontal stress and  $\sigma_{xx}$  is the horizontal

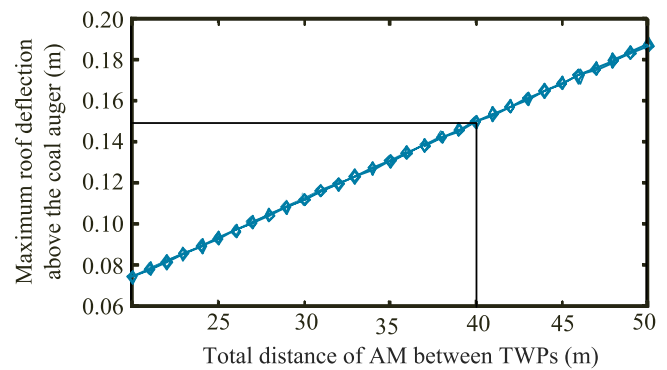


Figure 14. Relationship between the maximum roof deflection above the coal auger and total distance of AM between TWPs.

stress during the mining,  $\sigma_1$  and  $\sigma_3$  are the maximum and minimum principal stresses, MPa;  $k_{f0}$  is permeability when  $(\sigma_1 + \sigma_3)/2 = 1$  MPa.

#### 4.1. Stability of ICPs

The plastic zone and vertical stress distribution when the ICP width = 2 m at different mining stages are shown in figures 16 and 17, from which the following observations can be made:

- (1) When the AM work face advances 46 m, the plastic zone appears in No. 1 and No. 2 ICPs, suggesting they start to undergo the failure process.
- (2) When the AM work face advances 70 m, the plastic zone has covered No. 1, No. 2 and No. 3 ICPs, which indicates complete failure of these ICPs. The order of the pillar collapse is 2, 1 and 3. Note at this stage, No. 5 ICP must remain intact to support the roof in order to avoid the jamming of the auger drills.

The cases of AM with two different ICP widths were further analyzed and the results are shown in figure 18. Based on this figure, we can conclude that:

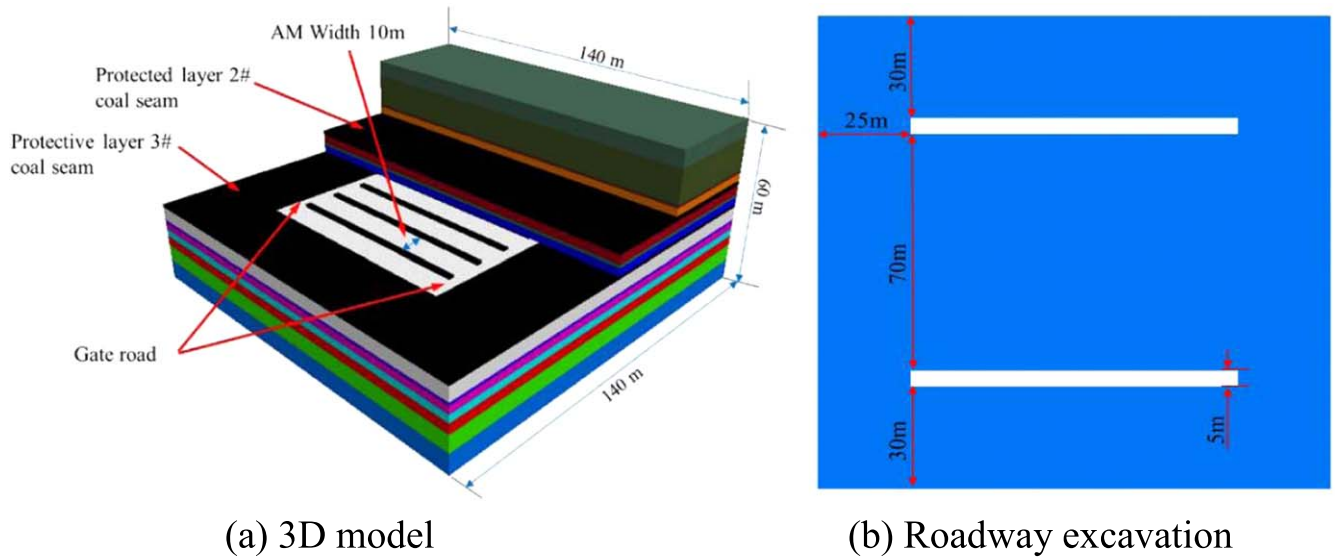


Figure 15. FLAC model of Chiyu Coal Mine.

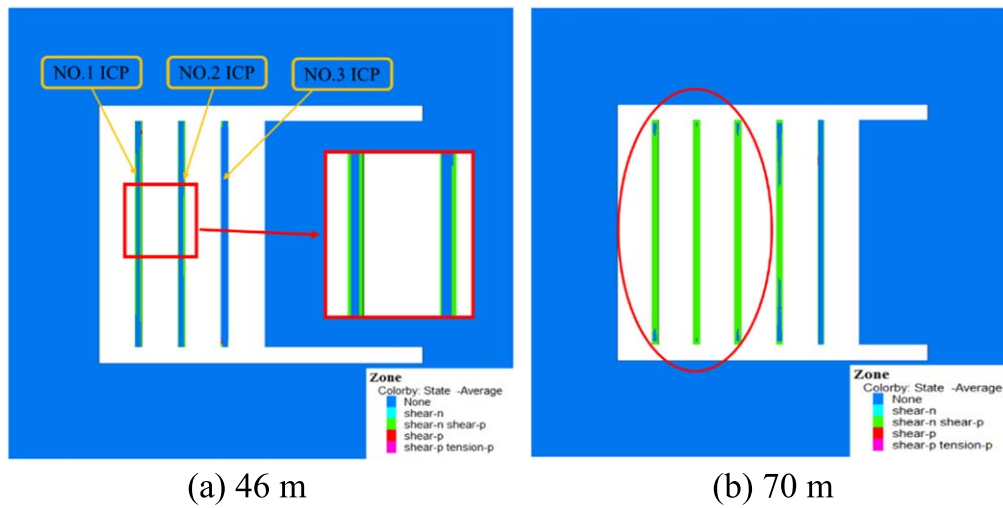


Figure 16. Plastic zone distribution at two different AM stages.

Table 1. Rock mechanical parameter.

Order	Lithology	Depth (m)	Density (kg m <sup>-3</sup> )	Bulk (GPa)	Shear (GPa)	Friction angle (°)	Cohesion (Mpa)	Tensile (Mpa)
1	Siltstone	7	2700	20.65	11.22	40	7	6.7
2	Sandy mudstone	12	2650	32.14	9.92	30	6.5	6.3
3	Mudstone	3.5	1800	15.55	4.05	28	5.5	5.3
4	4# coal	2.76	1450	13.33	4.44	32	5.2	2.0
5	Carbonaceous mudstone	2.5	1900	15.62	5.59	28	6	3.5
6	Medium fine sandstone	1.1	2600	22.54	8.64	35	6.8	5.2
7	Mudstone	4.89	1800	15.55	4.05	28	5.5	4.3
8	3# coal	1	1450	13.33	4.44	32	5.2	4.3
9	Siltstone	2.8	2700	20.65	11.22	40	7	4.0
10	Medium fine sandstone	1.1	2600	22.54	8.64	35	6.8	5.5
11	Mudstone	3.2	1800	13.33	4.11	28	5.5	5.0
12	2# coal	1.9	1450	13.33	4.44	32	5.2	2.0
13	Mudstone	2.8	1800	13.33	4.11	28	5.5	5.8
14	Medium fine sandstone	1	2600	22.54	8.64	35	6.8	7.2
15	Siltstone	12.2	2700	20.65	11.2	40	7	8.8
16	Medium fine sandstone	6.25	2600	22.54	8.64	35	6.8	10

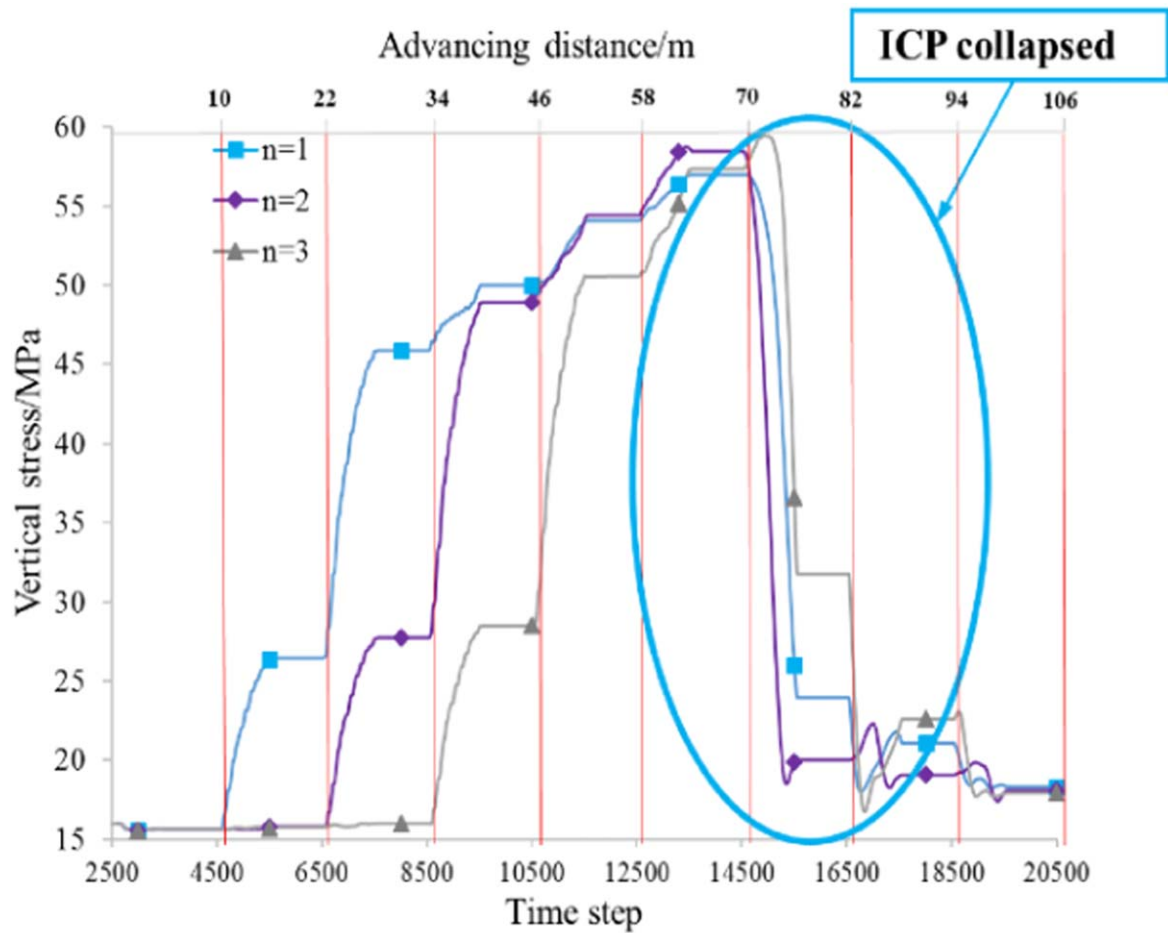
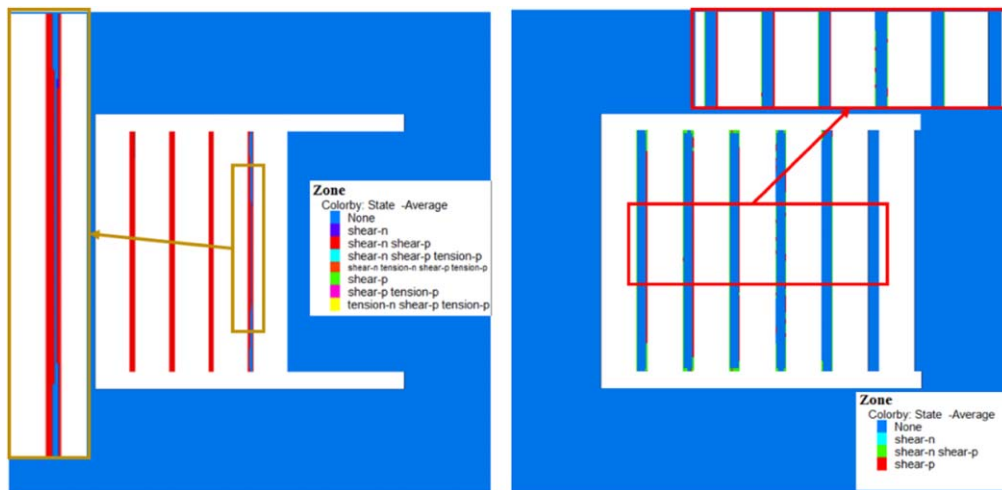


Figure 17. Vertical stress acting on ICPs at different AM stages.



(a) 1.5 m

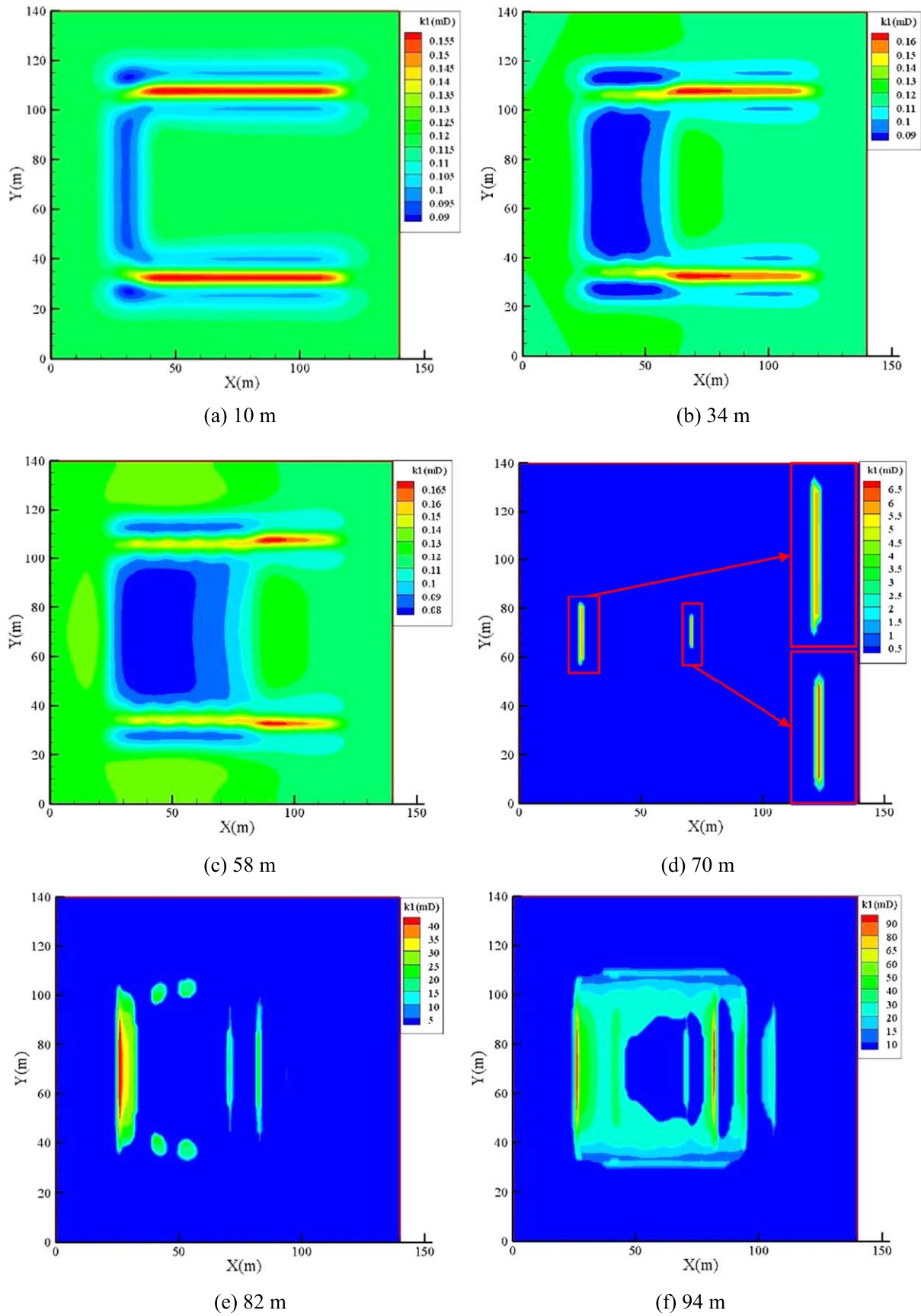
(b) 3.0 m

Figure 18. Plastic zone evolution with two different widths of ICPs.

(1) For ICP width = 1.5 m, once the AM work face advances 56 m, the ICPs will collapse, beginning with No. 2, followed by No. 1 and No. 3. No. 4 is partially covered by the plastic zone, suggesting it also suffers

from failure and therefore the coal auger may easily be jammed in place during operation.

(2) For ICP width = 3.0 m, some plastic zones just appear in part of the ICPs when the AM work face advances



Downloaded from https://academic.oup.com/jge/article/15/6/2626/5209788 by guest on 24 April 2024

Figure 19. Permeability evolution of 2# coal seam at different stages of mining of 3# coal seam using the proposed AM method.

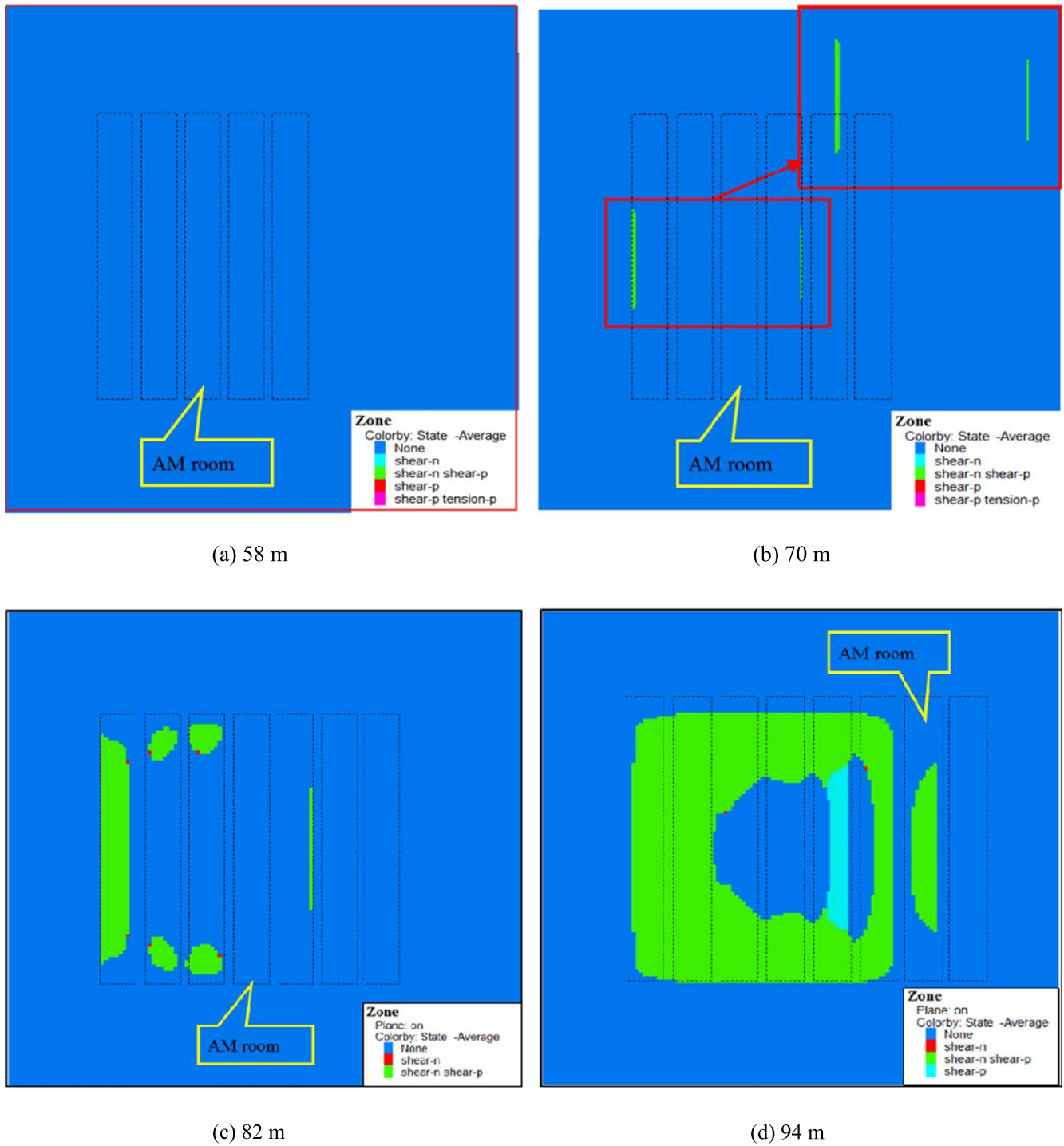


**Figure 20.** Development of plastic zones in 2# coal seam at different stages of mining of 3# coal seam using the proposed AM method.

88 m, indicating that the 3.0 m wide ICPs are strong enough to provide support to the roof for a long period of time.

- (3) It is therefore reasonable to conclude that for the case study of Chiyu Coal Mine, the width of the ICPs that meets the requirement of the proposed AM method is 2.0 m, as derived from the 2D studies.

#### 4.2. Permeability evolution in protected seam

The permeability evolution of 2# coal seam (protected layer) at different AM stages is shown in figure 19. The corresponding development of plastic zones within 2# coal seam is shown in figure 20.

The following observations can be made from figures 19 and 20:

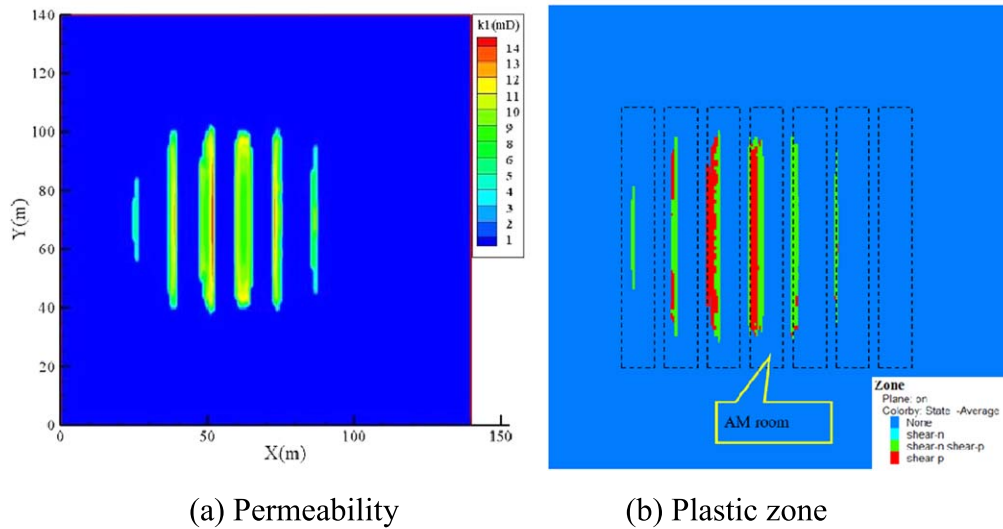


**Figure 21.** Permeability and plastic zone evolution of 2# coal seam when the ICP width is 3 m after the AM advancing distance reaches 88 m.

- (1) When the AM advancing distance is less than 58 m, the permeability of coal seam #2 only increases slightly with the maximum permeability of 0.165 mD (above the gate road), which is only 1.23 times the original permeability. The influence of AM on 2# coal seam is not significant at this stage and there is no plastic zone in the coal seam.
- (2) When the AM advancing distance reaches 70 m, the maximum permeability of 2# coal seam will increase to 6.72 mD, which is 50 times the original permeability. The sharp permeability increase is due to the plastic failure of 2# coal seam caused by AM in 3# coal seam. In a similar way, when the AM advancing distance reaches 82 and 94 m, the maximum permeability of 2# coal seam increases to 40 and 90 mD, respectively, which is 300 and 671 times the original value.

For the case when the ICP width = 3 m, as shown in figure 21, plastic failure zones only appear partially at two sides of some ICPs even after the AM advancing distance reaches 88 m. In this case, there is no complete failure of the ICPs and the permeability enhancement is not significant. The maximum permeability is 14 mD, which is 104 times the original permeability.

**4.3. Discussions**

- (1) Based on the numerical simulations presented above, ICPs with the width of 2.0 or 3.0 m can support the roof without complete failure during the AM process. However, the 2.0 m ICPs can provide temporary support and will collapse under the strata pressure after the AM advancing distance reaches a threshold distance, which satisfies the fundamental requirement of ICPs for the proposed AM method.
- (2) For permeability enhancement, the failure of ICPs can cause significant damage to surrounding rock and

enhance the permeability of protected layers. Therefore, the 2.0 m wide ICPs are suitable for the proposed AM method for pressure relief and permeability enhancement.

- (3) At present, AM has not been applied extensively in the filed due to the lack of mining equipment, but this method is verified in miniature. In the future, more large-scale validation will be carried out.

**5. Conclusions**

- (1) In order to ensure effective pressure relief and permeability enhancement on the protected layers when mining extremely thin coal seams underneath these layers, a more aggressive new AM method is introduced together with the process to optimize the key parameters such as AM room width, ICP width and the distance between adjacent TWPs.
- (2) The roof displacement increases significantly after the failure of ICPs. The required distance between adjacent TWPs is calculated based on the assumption of complete failure of all ICPs between them to ensure effective permeability enhancement. The value derived from numerical models and the theoretical analysis are in good agreement.
- (3) Numerical simulation results show that the failure of ICPs is guaranteed if designed properly so as to ensure effective pressure relief and permeability enhancement by AM. For the case study, the optimal width of ICPs to apply the proposed AM method is 2.0 m.
- (4) The proposed AM method in this paper is suitable for a coal seam group with extremely close distance due to the AM height. Theoretical analysis makes some assumptions, which may not be reasonable in some cases, such as very soft roof conditions.

## Acknowledgments

Financial support for this work was provided by the National Key R&D Program of China (No. 2018YFC0604701), the Natural Science Foundation of Jiangsu Province (No. BK20181358), the National Natural Science Foundation of China (No. 51404249), the Scholarship of the China Scholarship Council (CSC) and the Priority Academic Program Development of Jiangsu Higher Education Institutions.

## References

- Aguado M B D and Nicieza C G 2007 Control and prevention of gas outbursts in coal mines Riosa–Olloniego coalfield Spain *Int. J. Coal Geol.* **69** 253–66
- Bieniawski Z T 1968 *In situ* strength and deformation characteristics of coal *Eng. Geol.* **2** 325–40
- Chen C K, Lai H Y and Liu C C 2009 Application of hybrid differential transformation/finite difference method to nonlinear analysis of micro fixed-fixed beam *Microsyst. Technol.* **15** 813–20
- Chen H D, Cheng Y P, Zhou H X and Li W 2013 Damage and permeability development in coal during unloading *Rock Mech. Rock Eng.* **46** 1377–90
- Department of ship manufacturing Shanghai Jiao Tong University 2005 *Bending and Stability of Rod and Rod System* (Beijing: Science Education Press) pp 73–9
- Durucan S 1981 An investigation into the stress-permeability relationship of coals and flow patterns around working longwall faces *PhD Thesis* University of Nottingham
- Fang X Q, Zhao J J and He J 2009 Study on mining the protective seam with the manless working face in coal and gas outburst mines *Procedia Earth Planet. Sci.* **1** 227–34
- Jin K, Cheng Y, Wang W, Liu H, Liu Z and Zhang H 2016 Evaluation of the remote lower protective seam mining for coal mine gas control: a typical case study from the Zhuxianzhuang Coal Mine Huaibei Coalfield China *J. Nat. Gas Sci. Eng.* **33** 44–55
- Liu H and Cheng Y 2015 The elimination of coal and gas outburst disasters by long distance lower protective seam mining combined with stress-relief gas extraction in the Huaibei coal mine area *J. Nat. Gas Sci. Eng.* **27** 346–53
- Liu Y K, Zhou F B, Liu L, Liu C and Hu S Y 2011 An experimental and numerical investigation on the deformation of overlying coal seams above double-seam extraction for controlling coal mine methane emissions *Int. J. Coal Geol.* **87** 139–49
- Peng S P 2008 Present study and development trend of the deepen coal resource distribution and mining geologic evaluation *Coal* **7** 1–11
- Ranjith P G, Zhao J, Ju M, De Silva R V, Rathnaweera T D and Bandara A K 2017 *Opportunities and challenges in deep mining: a brief review Engineering* **3** 546–51
- Ren T X and Edwards J S 2002 Goaf gas modeling techniques to maximize methane capture from surface gob wells *Mine Ventilation* 279–86
- Song X P and Yun R G 2013 Design of high power shearer using for thin seam of 1 m minimum mining height *Coal Mine Machinery* **34** 1–2
- Swift G and Reddish D 2002 Stability problems associated with an abandoned ironstone mine *Bull. Eng. Geol. Environ.* **61** 227–39
- Tang Y 2015 Methane drainage optimization by roof-borehole based on physical simulation *Arabian J. Geosci.* **8** 7879–86
- Wang H F, Sun J Z, Chen Y P and Wei G J 2013a Theoretical thickness of protective layer mining and its application on pressure relief gas drainage *Electron. J. Geotech. Eng.* **18** 765–74
- Wang H, Cheng Y and Yuan L 2013b Gas outburst disasters and the mining technology of key protective seam in coal seam group in the Huainan coalfield *Nat. Hazards* **67** 763–82
- Wang S, Elsworth D and Liu J 2011 Permeability evolution in fractured coal: the roles of fracture geometry and water-content *Int. J. Coal Geol.* **87** 13–25
- Whittles D N, Lowndes I S, Kingman S W, Yates C and Jobling S 2006 Influence of geotechnical factors on gas flow experienced in a UK longwall coal mine panel *Int. J. Rock Mech. Min. Sci.* **43** 369–87
- Xiong Z Q, Wang C, Zhang N C and Tao G M 2015 A field investigation for overlying strata behaviour study during protective seam longwall over mining *Arabian J. Geosci.* **8** 7797–809
- Yan Y J and Miao L X 2009 Extremely thin protectors drilling picks the craft in protector mining application *Coal Technol.* **28** 9–10
- Yang T H, Xu T, Liu H Y, Tang C A, Shi B M and Yu Q X 2011 Stress–damage–flow coupling model and its application to pressure relief coal bed methane in deep coal seam *Int. J. Coal Geol.* **86** 357–66
- Yao B, Ma Q, Wei J, Ma J and Cai D 2016 Effect of protective coal seam mining and gas extraction on gas transport in a coal seam *Int. J. Min. Sci. Technol.* **26** 637–43
- Zhang C, Tu S, Bai Q, Yang G and Zhang L 2015 Evaluating pressure-relief mining performances based on surface gas venthole extraction data in longwall coal mines *J. Nat. Gas Sci. Eng.* **24** 431–40
- Zhang C, Tu S, Zhang L and Chen M 2016a A study on effect of seepage direction on permeability stress test *Arabian J. Sci. Eng.* **41** 1–14
- Zhang C, Tu S H, Zhang L, Bai Q S, Yuan Y and Wang F T 2016b A methodology for determining the evolution law of gob permeability and its distributions in longwall coal mines *J. Geophys. Eng.* **13** 181–93
- Zhou A, Wang K, Fan L and Kiryaeva T A 2017 Gas-solid coupling laws for deep high-gas coal seams *Int. J. Min. Sci. Technol.* **27** 675–9